Mathematical modelling and analysis of dynamic behaviour for seeded batch potash alum crystallization process

Cite as: AIP Conference Proceedings **2610**, 070005 (2022); https://doi.org/10.1063/5.0099958
Published Online: 29 August 2022

Siti Zubaidah Adnan and Noor Asma Fazli Abdul Samad

Mathematical Modelling and Analysis of Dynamic Behaviour for Seeded Batch Potash Alum Crystallization Process

Siti Zubaidah Adnan[1] and Noor Asma Fazli Abdul Samad[1,a)]

[1]*Chemical Engineering Department, College of Engineering, Universiti Malaysia Pahang, Lebuhraya Tun Razak, 26300 Kuantan Pahang, Malaysia*

[a)] *Corresponding author: asmafazli@ump.edu.my*

Abstract. Solubility phase diagram which consists of information on solute concentration, metastable and saturation limits against temperature, provides helpful insights in designing crystallization process to achieve desired crystal size distribution (CSD). Usually, the design of cooling crystallization process involves high supersaturation level at the beginning of the process in the metastable zone that is bounded by metastable and saturation limits. However, this high level of supersaturation causes an increment in both nucleation and crystal growth rates which induce the growth of the seed crystals as well as unwanted secondary nucleation that produce excessive fine crystals. Mitigation by employing proper temperature trajectory or policy along metastable zone to avoid unnecessary long operational time and fine crystals is needed. Thus, the purpose of this paper is to develop and simulate mathematical model of seeded batch crystallization process for the case of potash alum which is mainly used for purification in water treatment. Dynamic response of such process under open-loop operation for three cooling policies which are natural, linear and cubic is performed for evaluating the effect of different cooling policies on CSD. Simulation results based on the dynamic behaviour for all three cooling policies show cubic cooling policy obtained the best performance by achieving mean crystal size of 420 μm from the targeted CSD at 430 μm, and the mean crystal size for fine crystals is the lowest which is 35 μm compared to linear and natural cooling policies, at 40 μm and 55 μm, respectively. This information is prominent in deciding proper temperature trajectory of optimal cooling policy for potash alum crystallization process.

INTRODUCTION

Crystallization process is widely used in many industries especially in pharmaceuticals and specialty chemicals. Its capability to produce high quality of crystals makes it a beneficial and reliable process [1-2]. High quality of crystals is usually indicated by its conformity to crystal size, crystal shape, purity and a common control factor which is crystal size distribution (CSD). CSD is the main contributor that affects the bioavailability of the crystals, packing properties and the efficiency of the downstream operations [1-3]. Therefore, achieving high quality of crystal product is vital in the crystallization process.

In crystallization process, temperature is the main factor to be controlled for achieving desired CSD, since the solubility of the solution is defined as a function of temperature. Crystallization operation is usually started in the metastable or supersaturated zone with high level of supersaturation is expected due to high solute concentration in the solution. However, high level of supersaturation means high nucleation and crystal growth rate. This enables the seed crystals to grow due to high rate of crystal growth, but it also induces secondary nucleation that produce fine crystals. Additionally, crystallization operation that is operated in the metastable zone is restricted by saturation and metastable limits. Operation that is too close with any of these concentration limits may either cause longer operational time or uncontrolled excessive nucleation [4]. In the case of constant supersaturation policy where the supersaturation level is kept at minimum level to incite the growth of crystals while trying to reduce the nucleation effects, longer operational time is needed to complete each batch of production [5]. Usually, this operation takes twice longer than the normal operation time which is not economically feasible for industrial crystallizer. For the case of excessive

2nd Energy Security and Chemical Engineering Congress (ESChE 2021)
AIP Conf. Proc. 2610, 070005-1–070005-10; https://doi.org/10.1063/5.0099958
Published by AIP Publishing. 978-0-7354-4378-5/$30.00

nucleation where the process operates too close with metastable limit at the beginning of the process to achieve supersaturation state, the resulted unwanted fine crystals are laborious to mitigate where additional fines removal loop is needed to be employed [6-7]. Nonetheless, these issues may be overcome by employing temperature trajectory that is safely operated within saturation and metastable limits. Thus, sufficient knowledge on these crystallization mechanisms is required to determine the temperature trajectory inside the metastable zone.

Nevertheless, pioneer study that reported programmed cooling method provides better quality of the crystals, had established a significant impact on the study of optimal cooling profile to obtain desired CSD [8]. Subsequently, another study also implemented three cooling operating policies which are natural, linear, and cubic cooling for determining theoretical optimal cooling curves that correspond to desired CSD [9]. Natural cooling policy imitates the decreasing and concave up in temperature and is expected to have high nucleation rate due to high temperature gradient between coolant and solution at the beginning of crystallization operation. Linear cooling policy is referring to the decreasing of temperature at constant rate where the final CSD is projected to be superior to the CSD of natural cooling policy and closer to the CSD of cubic cooling policy. Meanwhile, cubic cooling policy shows decreasing and concave down profile in temperature where the idea is to keep the supersaturation level at constant and relatively low supersaturation [10]. Recent literatures used these cooling policies to analyse the outcome of crystallization process on CSD where cubic cooling policy undeniably provides better performance in supressing nucleation which give better morphology of the crystals and larger CSD [11-12]. Nevertheless, even after decades of optimizing cooling policy, these three cooling policies are still practical in providing better understanding of crystallization process and determining cooling rate that delivers better CSD hence the novelty of this study which is optimal cooling policy for the case for potash alum crystallization process.

In this study, the mathematical model and simulations of seeded batch crystallization process are developed and implemented in Matlab 2016b software. Potassium ammonium sulphate or potash alum crystallization process is used as a case study which is adapted from the literature [13]. The population balance equation (PBE) used to describe the process in the batch jacketed crystallizer is solved using method of classes (MOC) instead of combined quadrature method of moments (QMOM) and method of characteristics (MOCH) used by the literature for simpler computation. Then, dynamic responses of the specified crystallization process using three cooling policies in open-loop behaviour are analysed and validated against literature data [13]. The performance of natural, linear, and cubic cooling policies in terms of final CSD are further evaluated in the next section.

MATHEMATICAL MODELLING OF POTASH ALUM CRYSTALLIZATION

The mathematical model of seeded batch potash alum crystallization process is assumed to be one-dimensional and the crystals are grown based on the size dependent rate. Other than that, the mixture is assumed to be perfectly mixed in the batch jacketed crystallizer and secondary nucleation is considered in the process of crystallization. The main equation used in crystallization model known as population balance equation (PBE) which describes the behaviour of crystal population is shown in Equation (1) by neglecting the effects of agglomeration and breakage.

$$\frac{\partial n(L,t)}{\partial t} + \frac{\partial n(L,t)G(L,C,T)}{\partial L} = B_{nuc} \tag{1}$$

where n is the population density function (which is a function of particle size, L and crystallization time, t), G is the linear growth rate (which is a function of particle size, L, solute concentration, C, and solution crystallizer temperature, T in unit of μm/s), and B_{nuc} is the nucleation rate (number of particles/cm^3.min). This one-dimensional PBE which is in the form of partial differential equations (PDEs) are latter transformed into ordinary differential equations (ODEs) using method of classes instead of combined QMOM and MOCH as used in the literature for simpler yet sufficient solution of PBE (in terms of solution and complete retrieval of CSD) as shown in Equations (2) – (4).

$$\frac{dN_1}{dt} + \frac{G_{x1}}{2\Delta Cl_2}N_2 + \frac{G_{x1}-G_{x0}}{2\Delta Cl_1}N_1 = B_{nuc}, i = 1 \tag{2}$$

$$\frac{dN_i}{dt} + \frac{G_{xi}}{2\Delta Cl_{i+1}}N_{i+1} + \frac{G_{xi}-G_{xi-1}}{2\Delta Cl_i}N_i + \frac{G_{xi-1}}{2\Delta Cl_{i-1}}N_{i-1} = 0,\ 1 \le i \le n \tag{3}$$

$$\frac{dN_n}{dt} + \frac{G_x}{2\Delta Cl}N_n + \frac{G_x}{2\Delta Cl}N_{n-1} = 0,\ i = n \tag{4}$$

where N_i is the number of crystals per unit suspension for class I (number of particles/cm^3), G_x is the crystal growth rate in length direction x (μm/s), and ΔCl is the size of classes where $\Delta Cl=L_{xi}-L_{xi-1}$ (μm). The overall mass balance and energy balance for potash alum crystallization are shown in Equations (5) and (6), respectively.

$$\frac{dc}{dt} = -\frac{\rho_c k_v V}{m_w}\left(\sum_{i=1}^{i=N} S_{xi}^3 \frac{dN_i}{dt}\right) \tag{5}$$

$$\rho V c_p \frac{dT}{dt} = -\Delta H_c \rho_c k_v V \left(\sum_{i=1}^{i=N} S_{xi}^3 \frac{dN_i}{dt}\right) - U_1 A_1 (T - T_w) \tag{6}$$

where ρ_c is the crystal density (g/cm^3), k_v is the crystal shape factor, V is the volume of solution (cm^3), m_w is the mass of solvent (g), c_p is the heat capacity (J/g.°C), T is the temperature of the solution (°C), ΔH_c is the heat of crystallization (J/g), U_1 is the heat transfer coefficient of internal crystallizer (J/°C.min.cm^2), A_1 is the internal area of crystallizer (cm^2), and T_w is the cooling water temperature (°C). The saturation concentration, C_{sat} (g solute/g solvent) for potash alum is generated based on the following polynomial expression as the function of solution temperature from literature [13].

$$C_{sat} = 3.63 + 0.0243T + 0.00358T^2 \tag{7}$$

Next, the models for secondary nucleation and crystal growth in the power law form are shown in Equations (8) – (9):

$$B_{nuc} = k_b S^b V \tag{8}$$

$$G_{x_i} = k_g S^g \left(1 + \alpha_g L_{xi}\right) exp\, \beta_g \,, i = 1,2,3 \ldots n \tag{9}$$

where k_b and k_g, are the kinetic coefficients for nucleation and crystal growth respectively (number of particles/ cm^3.min). b and g are the nucleation order and crystal growth order, respectively. α_g and β_g are the crystal growth parameters. The relative supersaturation, S is applied as $S = (C - C_{sat})/C_{sat}$, and L_{xi} is the length of crystal particles (μm). Then, the total crystal mass, M_c (g) and crystal size distribution (CSD), f_n are calculated based on the following Equations (10) and (11), respectively.

$$M_c = \rho_c k_v (\sum_{i=1} S_{xi}^3 N_i) \tag{10}$$

$$f_n(L_{xi}) = \frac{1}{2}\left(\frac{N_i + N_{i+1}}{\Delta Cl}\right) \tag{11}$$

The initial seed distribution for this seeded operation and the targeted CSD profile are set at mean crystal size 90 μm and 430 μm, respectively which is similar to the literature [13]. The mean crystal size of both seed and targeted CSD as shown in **Error! Reference source not found.** is chosen for validation and demonstration purpose only and thus, other arbitrary size for seed and target can be chosen. Then, the performance of all cooling policies of natural, linear, and cubic are evaluated against the literature data that has been used as targeted CSD [13]. The calculation for percentage of error for validation against literature data is as shown in Equation (12).

$$\%\, of\ error = \frac{|Targeted\ CSD - Simulated\ CSD|}{Targeted\ CSD} \times 100 \tag{12}$$

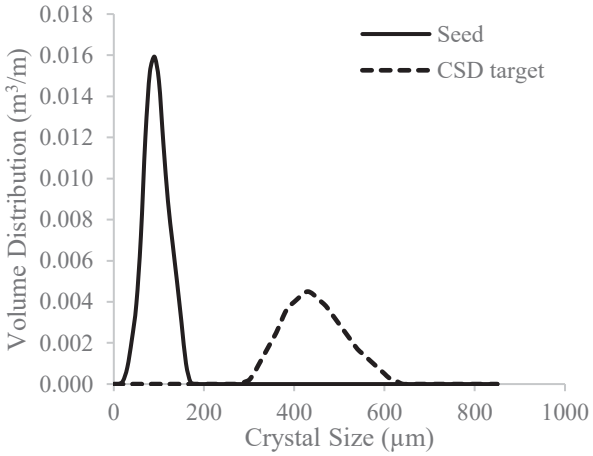

FIGURE 1. Initial seed and targeted final CSD

SIMULATION OF POTASH ALUM CRYSTALLIZATION PROCESS

The mathematical model as shown in Equations (2)-(11) for potash alum crystallization process is developed in Matlab 2016b software. The ODEs for this process are solved using backward Euler's method known as 'ode15s' solver in Matlab using the initial conditions in TABLE 1. The kinetic parameters used for this simulation are also tabulated in

TABLE **2** where both datasets are obtained from literature [13]. This simulation is divided for three parts which are natural, linear, and cubic cooling policies where each part represents different cooling trajectories for the same crystallization process. Then, the dynamic responses are compared between each cooling policy which are discussed further in the next section.

TABLE 1. Operating conditions based on [13]

Nomenclature		Values
T_{feed}	Saturation temperature of feed, ℃	40.0
T_{fin}	Final temperature, ℃	17.0
T_{batxh}	Batch time, min	90
L_s	Seed sieve size, µm	90-125
m_j	Mass of water in jacket, kg	10.738
C_o=C_{sat}(40 ℃)	Initial feed concentration, kg solute kg water $^{-1}$	0.104
ρ_c	Density, kgm^{-3}	1.75x10^3
k_v	Volumetric shape factor	0.62
c_{ps}	Heat capacity of slurry, Jkg^{-1}K^{-1}	1.4 x10^3
c_{pw}	Heat capacity of water, Jkg^{-1}K^{-1}	4.2 x10^3
ΔH_c	Heat of crystallization, Jkg^{-1}	2.0x10^5

TABLE 2. Value of kinetic parameters from [13]

Nomenclature		Values
k_b	Nucleation constant, µm^{-3}s^{-1}	0.0380
b	Nucleation order constant	3.4174
k_g	Growth constant, µms^{-1}	8.5708
g	Growth order constant	1.0000
α_g	Growth constant, µm^{-1}	0.0050
β_g	Growth constant	1.5777

ANALYSIS OF DYNAMIC BEHAVIOUR FOR POTASH ALUM CRYSTALLIZATION

Based on open-loop simulation results of seeded batch potash alum crystallization process, Fig. 2 (a) show the temperature profiles in the case of natural, linear, and cubic cooling policies respectively. For all three cases, the solution is cooled from 40 ℃ at the beginning of the process until it reached 17 ℃ at the end of the process. Temperature profile of natural cooling is declining rapidly following the decreasing concave up trend while for linear cooling profile, the temperature is decreasing linearly at constant rate. For cubic cooling profile, the temperature is following the concave down trend where the temperature is decreasing slowly until the end of crystallization process. These profiles from Fig. 2 (a) are the exact interpretation of the definition for natural, linear and cubic cooling policies based on published literatures [8-12].

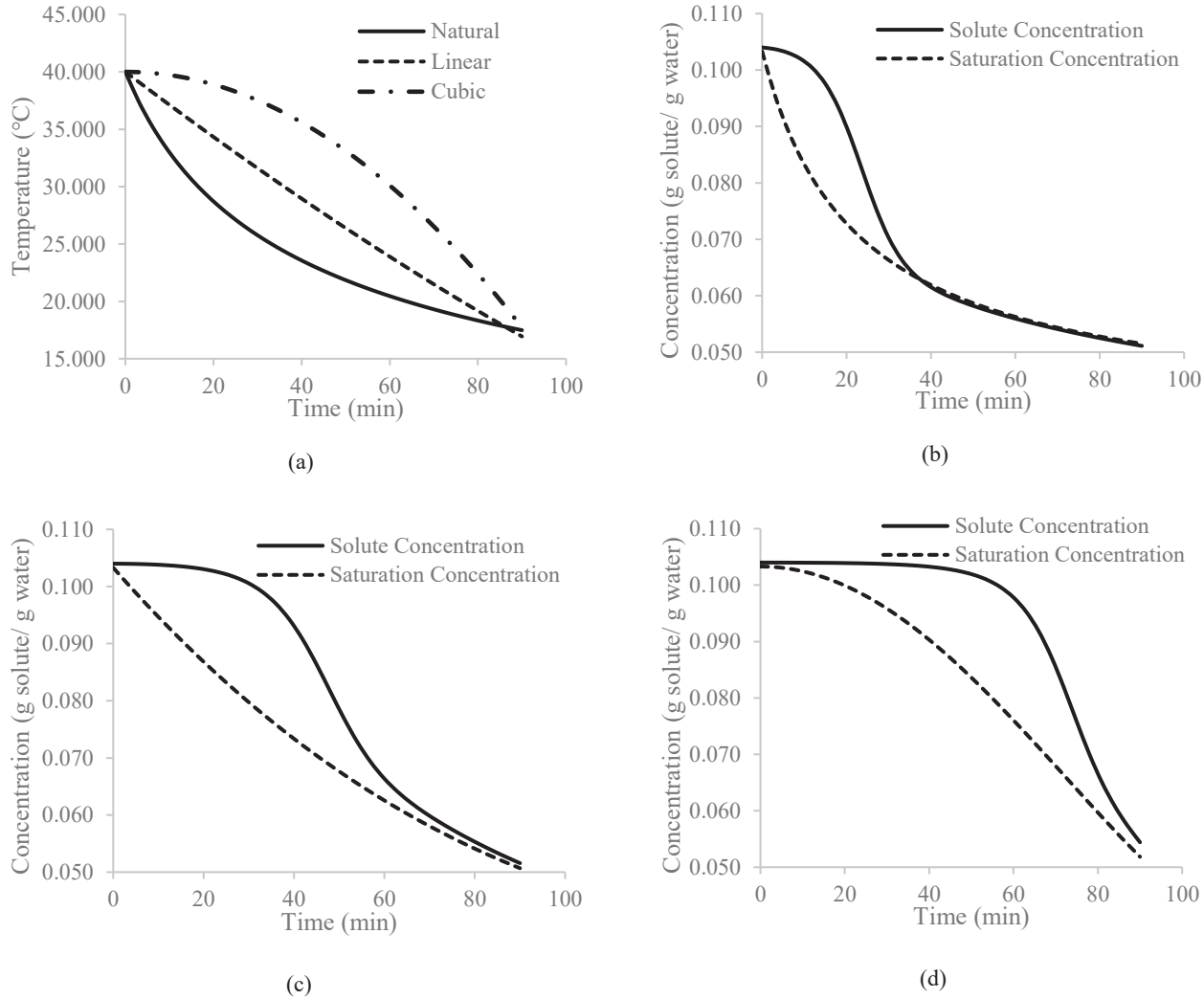

FIGURE 2. Temperature (a) and concentration profiles for natural (b), linear (c), and cubic (d) cooling policies

Next, Fig. 2 (b) demonstrates a steady drop of potash alum concentration (solid line) at the beginning of the process until 20 minutes of operation before it drops steeply from time 20 to 35 minutes. Then, it follows saturation concentration profile until the end of operation. The solute concentration for linear cooling policy, however, shows a 40-minute stable dropped before it was decreased steeply until it become saturated after 60 minutes of operation. This is shown by a solid line in Fig. 2 (c). Meanwhile, solid line in Fig. 2 (d) shows the solute concentration for cubic

cooling policy where it takes 60 minutes of gradual reduction in concentration before steeply decreasing until the end of process. All the concentration profiles from all cooling policies were dropped accordingly from 0.104 to 0.05 g of solute/ g of water and the saturation concentration profiles (dashed line) are following the descending trend of temperature profile indicating the relationship of concentration that depends on the temperature in which indirectly proved Equations (7).

Also, there is a huge gap between solute concentration and saturation concentration profiles, which define the supersaturation level for each cooling policy. For natural cooling policy, the huge gap between solute and saturation concentration profiles starts from time 0 until 40 minutes, and then it becomes saturated along the saturation limit from time 41 to 90 minutes. For linear cooling policy, the indication of high supersaturation level starts from 0 to 60 minutes and the solution becomes saturated after that specified operation time. Meanwhile, for cubic cooling policy the high supersaturation level starts from 20 until 80 minutes of process time and the solution is then become saturated, shortly after until the end of operation. These huge gaps between solute and saturation concentration profile or high supersaturation level in each cooling policy are clearly shown in Fig. 3 (a) where each supersaturation profile corresponds to the huge gap of solute concentration from saturation concentration at the different specific time of operation for all cooling policies. These gaps are expected to establish in order for crystallization to occur which is also describe in the literature where the gap between solute and saturation concentration will increase and eventually converge [14].

For natural cooling policy, the supersaturation profile shown in Fig. 3 (a) by the solid line showed that it reached its maximum value of 0.261at 15 minutes of operation which is corresponding to the huge gap of solute and saturation concentration during 0 to 40 minutes of operation. This indicates the active period for both nucleation and crystal growth rates as high supersaturation level promote the growth of seed crystals and formation of secondary nucleation. At the same time, it can be seen from Figs. 3 (b) and (c) that the nucleation and crystal growth rates reached its peak too. As the solution then become saturated from time 40 minutes until the end of operation, it can be observed that the supersaturation level reached zero, thus no visible effects on nucleation and crystal growth rates in Figs. 3 (b) and (c). Compared to all cooling policies, natural cooling policy is the highest in terms of nucleation rate but the lowest in crystal growth rate. This may be due to its temperature profile that decreased faster than other cooling strategies that imply no control on the dropped of temperature which causes higher nucleation rates at the beginning of the process than other cooling policies.

For linear cooling policy, the dashed line in Fig. 3 (a) shows the supersaturation level has reached its maximum value of 0.279 at 36 minutes of operation, within the same period of huge gap between solute and saturation concentration as observed in Fig. 2 (c). During this time, the increment of nucleation and crystal growth rates are also reported based on the dashed line in Figs. 3 (b) and (c). The nucleation rate shows by linear cooling policy is reduced by two third of nucleation rate for natural cooling policy. This relatively shows that linear cooling temperature trajectory could reduce the effects of secondary nucleation formed from high level of supersaturation. The peak of crystal growth rate of linear cooling policy is also slightly better than natural cooling policy which means that growth dominated process could be achieved by lowering the effects of nucleation. After 60 minutes of operation, due to the low supersaturation level at this time, no changes on the nucleation and crystal growth rate are noted.

Nonetheless, for cubic cooling policy, the supersaturation level shown by the dashed-dotted line in Fig. 3 (a) reached its maximum value 0.294 at 63 minutes of operation. This is consistent with the huge gap difference of solute and saturation concentration between 20 to 80 minutes of crystallization operation. Thus, it is demonstrated by Figs. 3 (b) and (c) that the nucleation and crystal growth rates increase around the same time. It is noted that the nucleation rate for cubic cooling policy is the lowest compared to natural and linear cooling policies. This may be due to its temperature profile that slowly drop at the beginning of the process to control the nucleation rate as the difference of solute concentration against saturation concentration is the highest at this time. Additionally, this slow dropped of temperature is an established method to control the high supersaturation level at the beginning of the process which contributes to the high nucleation and crystal growth rates and is proven experimentally in published literatures [8-12]. Also, the nucleation rate of cubic cooling policy did not start until it is 45 minutes of operation time which means that, the growth of the seed crystals is uninterrupted until 45 minutes of operation. This may also explain the reason of better crystal growth rate for cubic cooling policy compared to other cooling policies, as shown in Fig. 3 (c). The nucleation rate for cubic cooling policy suddenly increase in the middle of operation time may be due to the formation of secondary nucleation formed by the semi-ordered surface layers that is removed from the seed crystal's surface through fluid motion [15]. All in all, these results proved that supersaturation controls the nucleation and crystal growth rates that are responsible for the formation of new crystals and growth of seed crystals in which back up previous studies that uses supersaturation to control nucleation and crystal growth rate for better formation of CSD [1-14, 16].

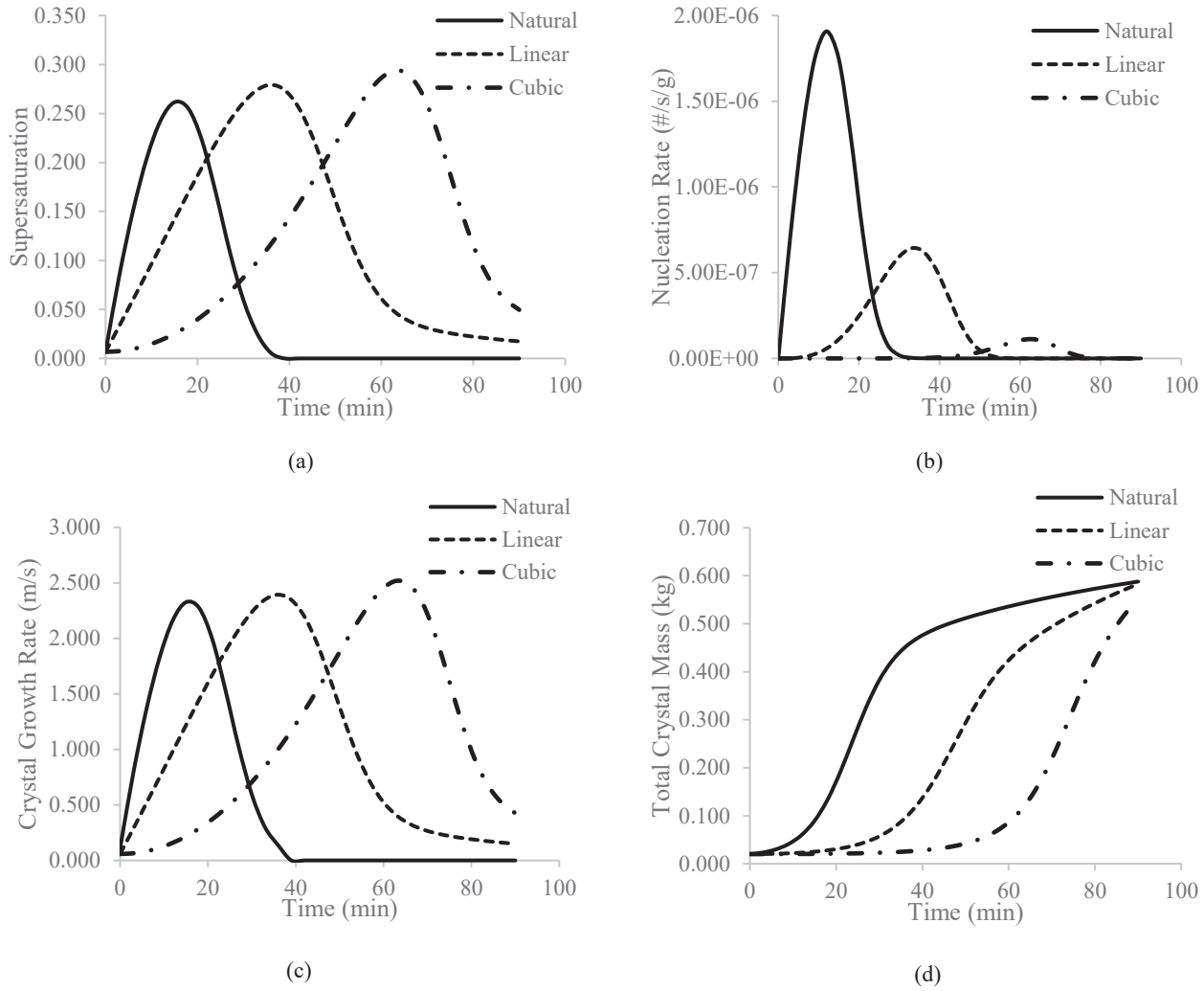

FIGURE 3. Supersaturation (a), nucleation rate (b), crystal growth rate (c), and total crystal mass profiles for natural, linear and cubic cooling policies

Next, Fig. 3 (d) shows the total crystal mass profile for all cooling policies which increases from 0.02 to 0.5 kg of potash alum crystals following the consequent effect of each policies' supersaturation level. All cooling policies produce almost similar total crystal mass due to the same amount of solute concentration is applied to all three cooling policies at the beginning of the process. Besides that, the impact of each cooling policy on the total crystal mass generated from seed crystals which represents mass of grown seed and fine crystals formed by secondary nucleation is clearly tabulated in TABLE 3. It is noted that the amount of total crystal mass generated from secondary nucleation for natural cooling policy is the worst, at 246 g and the generated mass of crystals in the case of cubic cooling policy is the least, at 49 g only. Same goes to the mass of crystal generated from the growth of the crystals where the cubic cooling policy is the best, at 491 g and the worst is in the case of natural cooling policy, at 329 g only. Linear cooling policy has total crystal mass closer to the cubic cooling policy which is 71 g generated from secondary nucleation and 490 g generated from growth of the seed crystals. These results are consistent with the published literature mentioned earlier where cubic cooling policy provides the best performance in overall quality [8-1210].

TABLE 3. Comparison of total crystal mass from nucleation and growth for all cooling policies

Cooling Policy	Total Crystal Mass (g)	
	Nucleation	Crystal Growth
Natural	246	329
Linear	71	490
Cubic	49	491

Lastly, final CSD profiles for natural, linear, and cubic cooling policies are plotted in Fig. 4 against targeted CSD that is adapted from literature [13] for validation purposes. It can be seen from Fig. 4 (a) that only CSD profile of cubic cooling policy almost reached the targeted CSD (430 μm), and natural cooling policy has the highest secondary peak compared to other profiles. From Fig. 4 (b) the CSD profile of natural cooling policy shows that the seed crystals did grow from mean crystal size of 90 μm to 340 μm, which is smaller by 90 μm than the mean crystal size of the targeted CSD, approximately. Also, the secondary peak which is grown in the size range of 0 to 160 μm is quite significant. Significant amounts of fine crystals generated from secondary nucleation during high level of supersaturation, may cause low purity and smaller final crystals [6]. The data from Fig. 4 (b) figuratively prove that statement.

For linear cooling policy, it can be observed from Fig. 4 (c) that the seed crystals have been grown from mean crystal size 90 μm to 380 μm which is a bit larger than the CSD profile for natural cooling policy. However, the final CSD for linear cooling policy still do not achieve the targeted CSD, smaller by mean crystal size 50 μm approximately. Other than that, the secondary peak which is ranging from 0 to 160 μm is also quite significant, however a bit less than the secondary peak of natural cooling profile. The height difference between primary peak of final CSD and initial seed CSD is because of the growth of crystals is assumed to be grown according to size dependent rate. Large crystals have higher crystal growth rate and vice versa, which resulted in producing a relatively low height of distribution [3].

Figure 4 (d) shows the final CSD of potash alum crystallization for cubic cooling policy. It is observed that the initial seeds have grown from mean crystal size 90 μm to 420 μm corresponds to the high level of nucleation and crystal growth rate as shown in Fig. 3 (b) and (c). It worth to note that the targeted CSD profile was almost achieved for cubic cooling policy. This may be due to the steep dropped in the temperature profile within 20 to 80 minutes of crystallization process that provide sufficient supersaturation level to induce the growth of seed crystals to achieve desired CSD. Apart from that, the amount of fine crystals in the secondary peak is still significant, even though the lowest compared to natural and linear cooling policy which can be seen in Fig. 4 (a). Therefore, it can be said that the final CSD profile of cubic cooling policy is the best between natural and linear cooling policies in which validated past research that agreed on the best cooling policy in terms of CSD is cubic [8-1210].

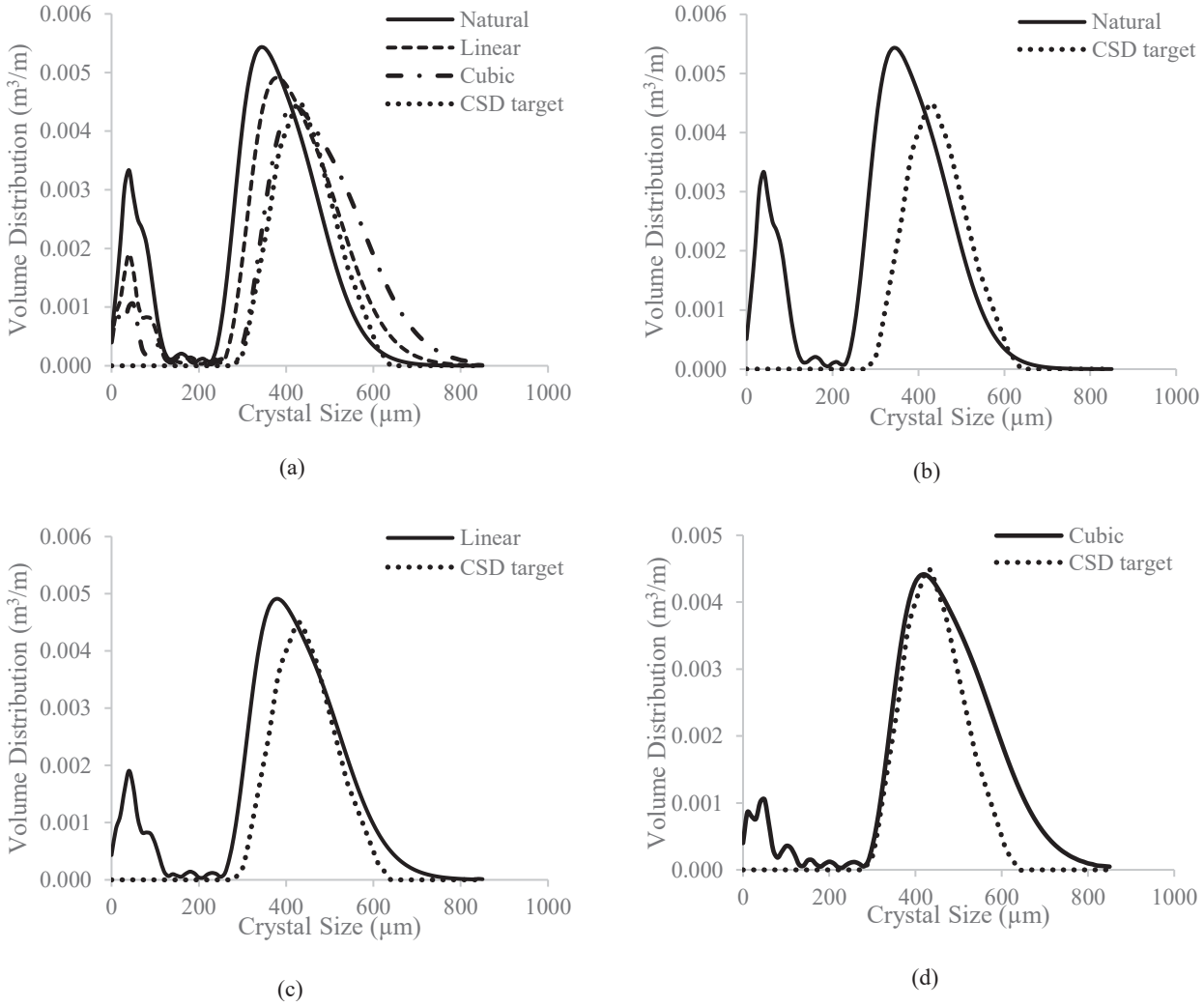

FIGURE 4. CSD profiles of all three cooling policies against targeted CSD (a), and CSD profile of natural (b), linear (c) and cubic (d) cooling policies against targeted CSD

Subsequently, TABLE 4 shows the performances of CSD profiles for all colling policies which are natural, linear, and cubic cooling in terms of mean crystal size which is the direct translation from Fig. 4 (a) where it is clearly observed that there are two peaks for the CSD profiles of each cooling policy. Primary peak is represented by mean crystal size that is larger than 200 μm while secondary peak is characterized by mean crystal size that is lower than 200 μm. From the tabulated data in TABLE 4, it is observed that the less performing cooling policy in terms of not achieving the targeted mean crystal size (which is 430 μm), and the highest mean crystal size of secondary peak is natural cooling policy. Significant amounts of fine crystals lead to smaller final CSD [6]. CSD profile for linear cooling policy is closer to cubic cooling policy with mean crystal size of 380 μm for primary peak and 40 μm for secondary peak which is in accordance with published literature [10]. Overall, cubic cooling policy has the best performance with the least amounts of fine crystals which is 420 μm and 35 μm for primary and secondary peak, respectively. This is because of the strategy of keeping low level of supersaturation at the beginning of the process that reduces the formation of fine crystals before ramping up the supersaturation level for sufficient growth of the seed crystals as suggested by published literatures [8-1210]. However, the formation of fine crystals from secondary nucleation which is induced by high level of supersaturation cannot be avoided as both nucleation rate and crystal growth rate depends on supersaturation level [15]. Other than that, cubic cooling policy has the lowest percentage of error against targeted CSD which is at 2.33%, to be compared with natural and linear cooling policies which are at 20.93% and 11.63%,

respectively. Therefore, these percentage of error against targeted CSD that are set based on CSD in literature [13], validated the results of this research where the best profile; cubic cooling policy has the least amount of error and fall below 5% of acceptance range of error based on standardized practice [17].

TABLE 4. Comparison of mean crystal size for all cooling policies

Cooling Policy	Mean Crystal Size (µm)	
	Primary Peak	Secondary Peak
Natural	340	55
Linear	380	40
Cubic	420	35

CONCLUSION

This paper discusses open-loop simulation for three cooling policies which is natural, linear, and cubic for seeded batch crystallization process using potash alum case study. The mathematical model based on population balance equation (PBE) was used to resemble batch jacketed crystallizer for the process in the Matlab software. The analysis of dynamic behaviour was conducted for all three cooling policies. From simulation results, cubic cooling temperature trajectory delivers the best performance in quality of final crystals. For mean crystal size of the primary peak, cubic cooling profile is 420 µm which is larger than natural and linear cooling profile at 340 µm and 380 µm, respectively. This means that its mean crystal size is the closest to the targeted CSD at 430 µm. In terms of secondary peak's mean crystal size, cubic cooling profile is at 35 µm which is lesser than natural and linear cooling profile at 55 µm and 40 µm, respectively. Therefore, the findings of this study validated past research and future work should be devoted towards another cooling strategy which uses dissolution phenomenon to obtain better temperature trajectory that minimize the effects of secondary nucleation.

ACKNOWLEDGEMENTS

The financial support provided by Universiti Malaysia Pahang (UMP) under Doctorate Research Scheme (DRS) is duly acknowledged.

REFERENCES

1. J. Unno and I. Hirasawa, Chem. Eng. Technol. **43**, 1065-71 (2020).
2. S. Z. Adnan and N. A. F. A. Samad, IOP Conf. Ser.: Mater. Sci. Eng. **702**, 012021 (2019).
3. M. Trampuž, D. Teslić, and B. Likozar, Powder Technol. **366**, 873-890 (2020).
4. S. Z. Adnan, S. Saleh, and N. A. F. A. Samad, AIP Conf. Proc. **2124**, 020042 (2019).
5. T. Zhang, B. Szilágyi, J. Gong, and Z. K. Nagy, AIChE J. **66**, 1-12 (2020).
6. Z. K. Nagy and E. Aamir, Chem. Eng. Sci. **84**, 656-70 (2012).
7. Z. K. Nagy, E. Aamir, and C. D. Rielly, Cryst. Growth Des. **11**, 2205-2219 (2011).
8. J. Mullin and J. Nývlt, Chem. Eng. Sci. **26**, 369-77 (1971).
9. A. Jones, Chem. Eng. Sci. **29**, 1075-87 (1974).
10. H. Hojjati and S. Rohani, Chem. Eng. Process. **44**, 949-957 (2005).
11. D. Zhang, L. Liu, S. Xu, S. Du, W. Dong, and J. Gong, J. Cryst. Growth **486**, 1-9 (2018).
12. M. Lenka and D. Sarkar, Powder Technol. **334**, 106-116 (2018).
13. E. Aamir, "Population balance model-based optimal control of batch crystallisation processes for systematic crystal size distribution design," Ph.D. thesis, Loughborough University, 2010.
14. F. Montes, K. Gernaey, and G. Sin, Ind. Eng. Chem. Res. **57**, 10026-10037 (2018).
15. D. Erdemir, A. Lee, and A. Myerson, *Handbook of Industrial Crystallization* (Cambridge University Press, Cambridge, 2019), p. 76.
16. B. Szilagyi, A. Eren, J. L. Quon, C. D. Papageorgiou, and Z. K. Nagy, Cryst. Growth Des. **20**, 3979-3996 (2020).
17. S. Samsuri, N. L. Jian, F. W. Jusoh, E. H. Yáñez, and N. Y. Yahya, Chem. Eng. Technol. **43**, 447-456 (2020).